Available online at www.sciencedirect.com
SCIENCE DIRECT®
International Journal of Heat and Mass Transfer 48 (2005) 3516–3526
International Journal of HEAT and MASS TRANSFER
www.elsevier.com/locate/ijhmt

# Molecular dynamics simulation of a thin water layer evaporation and evaporation coefficient

T.H. Yang, Chin Pan *

*Department of Engineering and System Science, National Tsing Hua University, Hsinchu 30043, Taiwan, ROC*

Received 28 September 2004; received in revised form 24 March 2005
Available online 23 May 2005

**Abstract**

This work investigates the evaporation of a thin water layer into vacuum using molecular dynamics simulations based on TIP4P model for intermolecular potential. The results of simulation reveal micro-scale physical phenomena near the liquid–vapor interface such as evaporation, condensation, recoil after evaporation or condensation, and molecular exchanges. The simulations show that the hydrogen bond has a significant effect on the molecular behavior near the interface and may reduce the evaporation coefficient. This study also demonstrates that the combination of molecular dynamics simulations and the classical Schrage model may provide an elegant methodology to determine the evaporation coefficient of water at different temperatures or corresponding saturation pressures.


## 1. Introduction

Interfacial heat and mass transfer are the key elements of various phase-change problems and are of significant fundamental importance for both science and engineering applications. There have been numerous studies in the literature since the pioneering work of Hertz and Knudsen on the evaporation of liquid mercury into vacuum. The evaporation flux may be predicted by the Hertz–Knudsen–Schrage equation or its modified form. However, an accurate prediction of evaporation flux at an interface by the model has been hampered by the uncertainty in the numerical values of the evaporation or condensation coefficients and the determination of external states [1]. This is particular the case for water. A recent analysis given by Marek and Straub [2] of both theoretical predictions and experimental data indicated that for water, a polar substance, the deviation of evaporation coefficient or condensation coefficient is two to three orders of magnitude. The experimental determination of evaporation coefficient or condensation coefficient is quite difficult "as the temperature at the interface, which jumps within a few molecule layers, cannot directly be measured" [2].

Recently, molecular dynamics (MD) simulations have been employed in the literature to determine the evaporation or condensation coefficient as well as the rate of phase change at the interface [3]. For example, Yasuoka and Matsumoto [4] employed MD simulation to obtain the condensation coefficient of argon, methanol and water at certain temperatures. Matsumoto [5] employed molecular dynamics simulation to explore the evaporation–condensation dynamics of pure fluids under both equilibrium and non-equilibrium conditions. Wu and Pan [6] investigated the evaporation of a thin

* Corresponding author. Tel.: +886 3 5725363; fax: +886 3 5720724.
*E-mail address:* cpan@ess.nthu.edu.tw (C. Pan).

0017-9310/$ - see front matter © 2005 Elsevier Ltd. All rights reserved.
doi:10.1016/j.ijheatmasstransfer.2005.03.015

**Nomenclature**

| | |
|---|---|
| $A_i$ | interfacial area ($m^2$) |
| $\vec{a}_i$ | acceleration vector of $i$th molecule ($m\ s^{-2}$) |
| $C_1$ | fitted constant in Eq. (7) ($Å^{-3}$) |
| $C_2$ | fitted constant in Eq. (7) ($ps^{-1}$) |
| $d$ | fitted constant in Eq. (3) (Å) |
| $E_{ki}$ | kinetic energy of $i$th molecule (J) |
| $e$ | elementary charge (C) |
| $\vec{F}_i$ | total force vector acting on $i$th molecule (N) |
| $j_-$ | condensation mass flux ($m^{-2}\ s^{-1}$) |
| $j_+$ | evaporation mass flux ($m^{-2}\ s^{-1}$) |
| $k_B$ | Boltzmann constant ($J\ K^{-1}$) |
| $L_x$ | length of the simulation box in the $x$-direction (Å) |
| $L_y$ | length of the simulation box in the $y$-direction (Å) |
| $L_z$ | length of the simulation box in the $z$-direction (Å) |
| $M$ | molecular weight ($kg\ mol^{-1}$) |
| $m_i$ | mass of $i$th molecule (kg) |
| $N$ | number of molecules in the simulation system |
| $N_L$ | number of molecules in the liquid region or interface layer |
| $n$ | coordination number of hydrogen bond per water molecule |
| $n(t)$ | time evolution of molecular number density in the vapor side ($Å^{-3}$) |
| $P_L$ | saturation pressure at interfacial temperature (Pa) |
| $q_{ia}$ | charge on the site $a$ of $i$th molecule (C) |
| $q_{jb}$ | charge on the site $b$ of $j$th molecule (C) |
| $P(n)$ | possibility of coordination number |
| $R$ | universal gas constant ($J\ mol^{-1}\ K^{-1}$) |
| $r_{cut}$ | cut-off distance between two water molecules (Å) |
| $r_{iajb}$ | distance between site $a$ of $i$th molecule and site $b$ of $j$th molecule (Å) |
| $\vec{r}_{ij}$ | position vector between $i$th molecule and $j$th molecule (Å) |
| $r_{ij}$ | distance between $i$th molecule and $j$th molecule (Å) |
| $r_{OH}$ | distance between two sites of oxygen and hydrogen in a molecule (Å) |
| $r_{OM}$ | distance between two sites of oxygen and negative charge in a molecule (Å) |
| $T$ | temperature (K) |
| $T_L$ | liquid or interface temperature (K) |
| $t$ | simulation time (ps) |
| $V$ | volume of the vapor side ($m^3$) |
| $z_0$ | position of the Gibbs dividing surface (Å) |
| *Greek symbols* | |
| $\delta$ | interfacial thickness (Å) |
| $\varepsilon_{oo}$ | characteristic length of Lennard-Jones parameters for oxygen pairs (J) |
| $\varepsilon_0$ | permittivity (dielectric constant) in vacuum ($C^2\ s^2\ m^{-3}\ kg^{-1}$) |
| $\pi$ | ratio of the circumference of a circle to its diameter |
| $\rho_L$ | liquid density ($kg\ m^{-3}$) |
| $\rho_V$ | vapor density ($kg\ m^{-3}$) |
| $\sigma_{oo}$ | characteristic energy of Lennard-Jones parameters for oxygen pairs (Å) |
| $\sigma_e$ | evaporation coefficient |
| $\sigma_c$ | condensation coefficient |
| $\phi_{ij}$ | effective pair potential between molecule $i$ and molecule $j$ (J) |

argon layer into vacuum using molecular dynamics simulations based on the Lennard-Jones potential. Considering the balance of vapor molecules and combining with the Schrage model, they were able to derive an equation for the evaporation coefficient based on a fitted equation from the simulation results.

Molecular dynamics simulations have also been applied to other phase-change problems. For example, Yi et al. [7] conducted molecular dynamics simulation of an ultra-thin liquid argon layer (2 nm) on a platinum surface. They found that the simulation results agree with the vaporization process of a similar macroscopic system. At moderate wall temperatures gradual evaporation process takes place, while at high surface temperatures a vapor region is formed between the surface and the liquid mass, which is really the Leidenfrost phenomenon. Wu and Pan [8] investigated bubble nucleation based on molecular dynamics simulations in a homogeneous Lennard-Jones liquid under heating with a constant mean negative pressure. The simulated nucleation rates agreed very well with the predictions of classical theory. Depending on the pressure, the bubble growth rates from the simulation were from 0.08 to 0.197 Å $ps^{-1}$, about one order of magnitude smaller than that predicted by the Rayleigh equation.

The present work employs molecular dynamics simulations based on the TIP4P potential to investigate the mechanisms of evaporation of thin water film into vacuum. Following a similar approach proposed by Wu and Pan [6], the evaporation coefficients of water are determined at various different pressures and compare with theoretical predictions in the literatures.

## 2. Simulation models and procedure

The molecular dynamics method is based on the classical Newton's second law of motion. Following the derivation of the Hamiltonian dynamics, the equation of motion for each atom or molecule under consideration may be expressed as [9]:

$$\vec{F}_i = m_i \vec{a}_i = m_i \frac{\mathrm{d}^2 \vec{r}_i}{\mathrm{d}t^2} = \sum_{j \neq i}^{N} -\frac{\mathrm{d}\phi_{ij}(r)}{\mathrm{d}r} \frac{\vec{r}_{ij}}{r_{ij}} \tag{1}$$

where $\vec{F}_i$ is the total force vector acting on the $i$th molecule; $N$ is the number of molecules; $\phi_{ij}$ is the pair potential between the $i$th molecule and $j$th molecule; $\vec{r}_{ij}$ represents the position vector and $r_{ij}$ is the distance between $i$th molecule and $j$th molecule; $m_i$ is the mass of $i$th molecule; $\vec{a}_i$ is the acceleration vector of $i$th molecule.

The TIP4P model was adopted as the effective pair potential between water molecules. The model consists of four sites: two of them for positive charged hydrogen atoms, one negative charged site for the oxygen atom, and another Lennard-Jones site for the oxygen atom [10]:

$$\phi_{ij} = 4\varepsilon_{\mathrm{oo}} \left[ \left( \frac{\sigma_{\mathrm{oo}}}{r_{iajb}} \right)^{12} - \left( \frac{\sigma_{\mathrm{oo}}}{r_{iajb}} \right)^{6} \right]_{\substack{a=1 \\ b=1}} + \sum_{a=2}^{4} \sum_{b=2}^{4} \frac{q_{ia} q_{jb}}{4\pi\varepsilon_0} \frac{1}{r_{iajb}} \tag{2}$$

where $\phi_{ij}$ is the effective pair potential for water between molecule $i$ and molecule $j$; $\varepsilon_{\mathrm{oo}}$ and $\sigma_{\mathrm{oo}}$ are the Lennard-Jones parameters for oxygen pairs; $\varepsilon_0$ is the dielectric constant; $r_{iajb}$ stands for the distance between site $a$ and site $b$; $q_{ia}$ and $q_{jb}$ represents the charges on site $a$ and site $b$, respectively. The numerical values of these parameters for TIP4P are listed in Table 1. The cut-off distance employed in the simulation was 9.0 Å. The TIP4P potential is an effective pair potential optimized based on the thermodynamic data of liquid water [10]. Its application to the vapor–liquid interface is examined by comparing simulated liquid and vapor densities with tabulated data from the literature and predictions from other potential models later in Fig. 4 and associate discussion.

Table 1
Numerical values of parameters in TIP4P of water [10]

| Parameters | TIP4P |
|---|---|
| $\varepsilon_{\mathrm{oo}}$ (J) | $1.077 \times 10^{-21}$ |
| $\sigma_{\mathrm{oo}}$ (Å) | 3.154 |
| $r_{\mathrm{OH}}$ (Å) | 0.957 |
| $r_{\mathrm{OM}}$ (Å) | 0.15 |
| ∠HOH (°) | 104.52 |
| $q_{\mathrm{H}}$ (C) | 0.52e |
| $q_{\mathrm{M}}$ (C) | −1.04e |

The simulation system for the evaporation of a water film was a parallelopiped with the water film in the middle of the $z$-axis as shown in Fig. 1. A total of 1000 water molecules initially with a fcc arrangement with dimension in the $x$–$y$ plane of about $25 \times 25$ (Å)$^2$. This dimension may be slightly changed at different temperatures to account for density variation with temperature with the initial fcc structure. The liquid layer thickness is equivalent to the density corresponding to the initial temperature specified. The length in the $z$-direction was 150 Å. The periodic boundary condition was applied for all the six boundaries.

The numerical integration for the system of equations employed Gear's predictor–corrector algorithm. In order to improve computation performance and save computing time, the computation of interactions between molecules employed the neighbor-list method and the programming procedure was paralleled by MPI FORTRAN 77/90 on IBM p690 workstations.

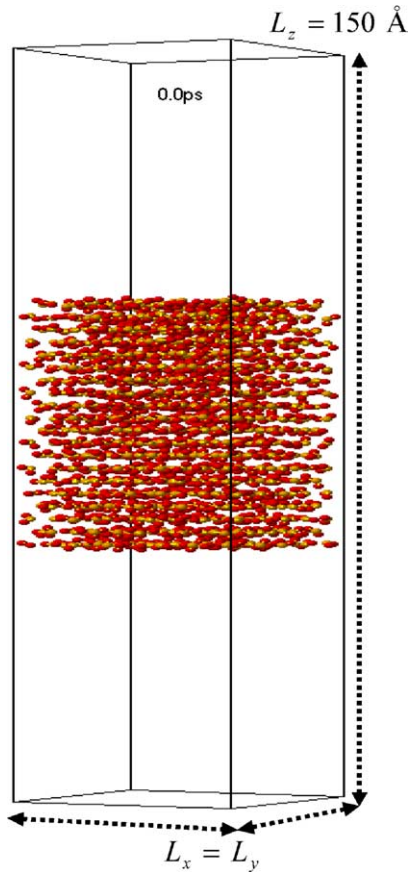


Fig. 1. Simulation model for evaporation of a thin water layer.

## 3. Results and discussion

### 3.1. Liquid–vapor interfacial region

The interfacial region is the key stage for phase-change phenomena to play and, therefore, deserves detail examinations. The interfacial region is a narrow space with density changes continuously, though very sharp in fact, from the liquid density to the vapor one. Fig. 2(a) displays the density distributions for several different temperatures in the direction normal to the interface after the system reaches the equilibrium state. The figure clearly demonstrates three distinct regions, namely, liquid layer, transition layer, and vapor zone. As suggested by Chapela et al. [14], the density profile across the three regions may be fitted very well (see Fig. 2(b)) by a hyperbolic-tangent function:

$$\rho(z) = \frac{1}{2}(\rho_L + \rho_V) - \frac{1}{2}(\rho_L - \rho_V) \times \tanh\left[\frac{z - z_0}{d}\right] \quad (3)$$

where $\rho_L$ and $\rho_V$ are the liquid and vapor densities, respectively; $z_0$ is the position of the Gibbs dividing surface [13], $d$ is a measure of the interfacial thickness and is related to the interfacial thickness as

$$\delta = 2.1792d \quad (4)$$

The interfacial thickness is from 4 to 8 Å and increases approximately with increasing the temperature. Fig. 3 shows that the interfacial thickness may be fitted very well with the temperature of the form:

$$\delta = -10.95 + 0.04068T \quad (5)$$

where $\delta$ is in Å and $T$ is in K. The interfacial thickness for water is much smaller than that for argon, which is from 16 to 20 Å [6].

The simulated liquid and vapor densities agree fairly well with tabulated data [11] and molecular simulations with other potential models [12,13], as shown in Fig. 4. The simulated data of the present study based on the TIP4P model for the liquid water density under-predict the tabulated values from 3% to 10% and the deviation increases with increasing the temperature. The relative deviation for the vapor density, however, is much larger, from 100% to 200%. This suggests the limitations of the TIP4P model and other currently available potential models for water.

Significant temperature fluctuations are present in the liquid region as well as the interfacial area as shown in Fig. 5 for water at 463.15 K. The temperature for the liquid region or interface layer, $T_L$, is evaluated by the mean kinetic energy of the group of molecules in the liquid region or interface layer as:

$$T_L = \frac{2}{3k_B N_L} \sum_{i=1}^{N_L} E_{ki} \quad (6)$$

where $E_{ki}$ is the kinetic energy of molecule $i$, $N_L$ is the total number of molecules in the liquid region or interface layer, $k_B$ is the Boltzmann constant. The temperature fluctuation is primarily due to the velocity

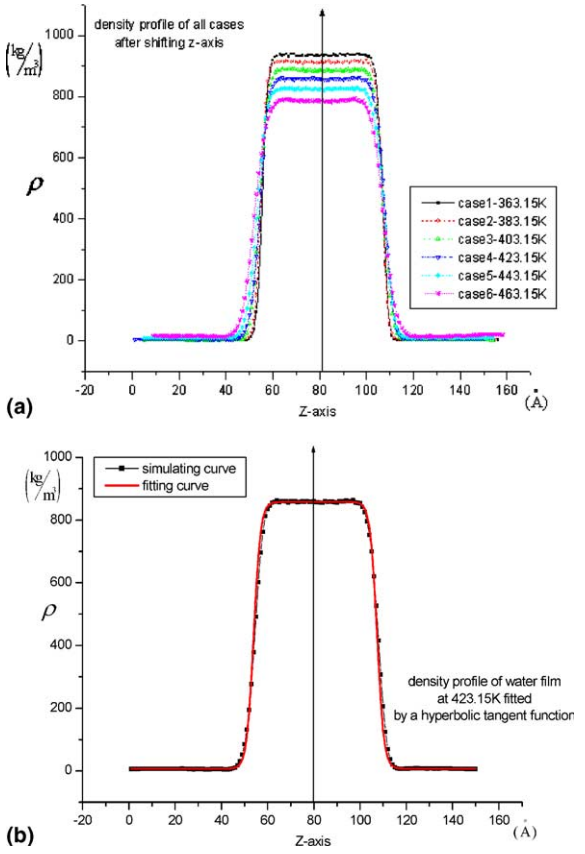


Fig. 2. (a) Density profile at various different temperatures. (b) Density profile at 423.15 K and its fitted curve of hyperbolic tangent form.

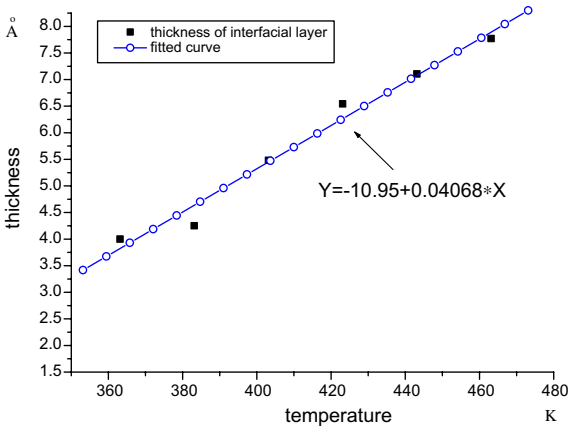


Fig. 3. Thickness of the interfacial region as a function of temperature.

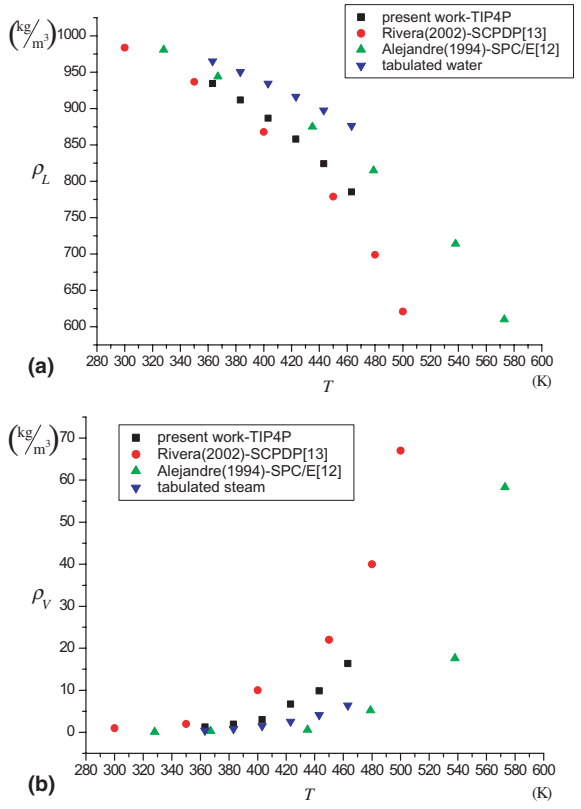


Fig. 4. Comparison of simulated density with tabulated data and simulated results from literature (a) liquid density and (b) vapor density.

distribution of liquid molecules and a relatively small number of molecules under simulation. The temperature fluctuation at the interface can be as high as 30 K for this case, while it is less than 10 K for the liquid layer. The temperature fluctuations in the interface region are much more violent than that inside the liquid layer, because the molecules in the interface region are less constraint than those inside the liquid. Moreover, the number of molecules in the interface layer is only 62–119 molecules, depending on temperature, which is much smaller than that in the liquid region, from about 600 to 800 molecules. Such a small number of molecules in the simulated system may also be a reason for the significant temperature fluctuations in the interface layer. On the other hand, evaporation at the interface is basically escape of more energetic, vapor-like, molecules from the interface to the vapor side; consequently, the mean temperature for the interface region is about 5 K smaller than the liquid temperature inside. The slight temperature reduction at the interface during evaporation is usually attributed to the cooling effect of evaporation macroscopically. The molecular dynamics simulations provide a more insightful observation. The simulation for argon system also presented the similar results [6].

### 3.2. Molecular behavior near or at the interface

Molecular simulations allow direct numerical visualization of molecular behavior near the interface. Using the PV-WIN to show the results from molecular simulations, the molecular behavior near or in the interfacial region is investigated in what follows. To make visualization clearly, only 300 molecules near the interface are observed and for the figure to be shown in this section, the sphere represents the oxygen atom, while the tips of two sticks on the sphere stand for the two hydrogen atoms respectively.

Evaporation, i.e., a molecule emitting from the interface region to the vapor one, and condensation, i.e., a vapor molecule impinging the interface region and staying there or further inside, are two fundamental mechanisms near the interface. A molecule in the liquid region may gain energy from a series of collisions, in fact,

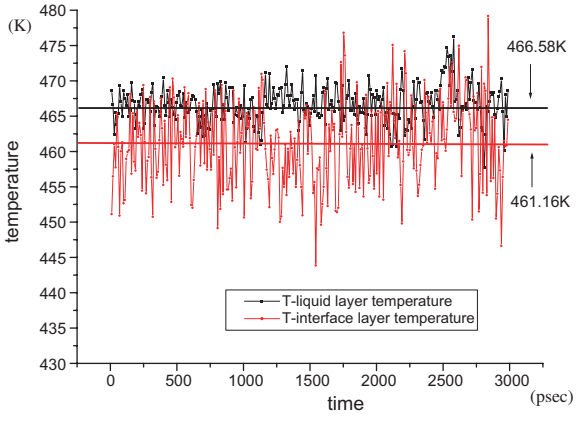


Fig. 5. Significant temperature fluctuations of liquid and interfacial temperatures.

interactions with other molecules and eventually evaporates into the vapor region. On the other hand, a vapor molecule may also condense into the liquid film.

Other than condensation mechanism describe above, a high speed vapor molecule may recoil to vapor region again after it "collide" with a molecule or molecules in the interface region. Fig. 6 illustrates that No. 127 molecule collides with No. 664 at $t = 52.3$ ps. At $t = 53.3$ ps, No. 127 molecule is back to the vapor region and moving away. On the other hand, a molecule just evaporated with high speed may collide with a molecule in the vapor region and recoil to the interface region again. Fig. 7 displays that No. 400 molecule collides with No. 721 at 439.2 ps. After about 3 ps of interactions, No. 400 molecule is moving back to the interface region, while No. 721 molecule is traveling away from the interface.

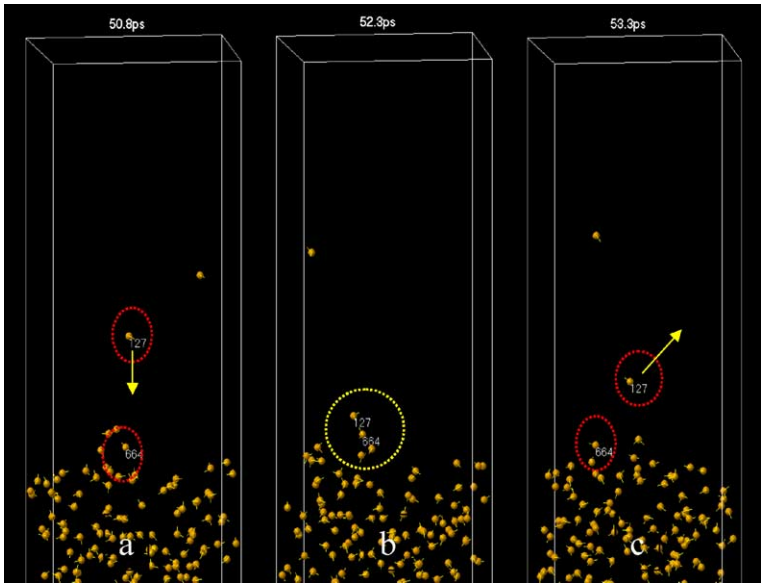


Fig. 6. Collision and recoil of a vapor molecule with interfacial molecules.

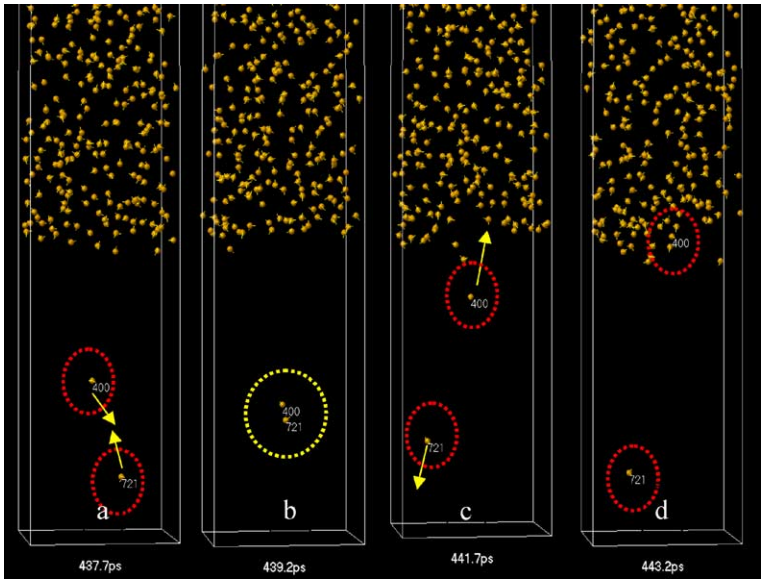


Fig. 7. Condensation due to the collision of two vapor molecules.

Moreover, for the water system, the hydrogen bound may play a significant role for the molecular behavior near the interface. A just evaporated molecule may be recaptured by the nearby molecules in the interfacial region through hydrogen bonds between the molecule under consideration and nearby molecules in the interfacial region. Fig. 8 demonstrates such an effect. At 16.9 ps, No. 697, 775 and 871 molecules are next each other and all in the interface region. At 19.4 ps, No. 775 molecule evaporates and is moving away from the interface slowly. At 19.9 ps, a hydrogen bond is formed between No. 775 and No. 871 and No. 775 is attracted toward the interface. At 20.4 ps, another hydrogen bond is formed between No. 775 and No. 697. At 25.4 ps, No. 775 is back to the interface region again. This demonstrates that the hydrogen bond effect due to the polar structure of a water molecule may effectively reduce the evaporation effect. Moreover, such a kind of

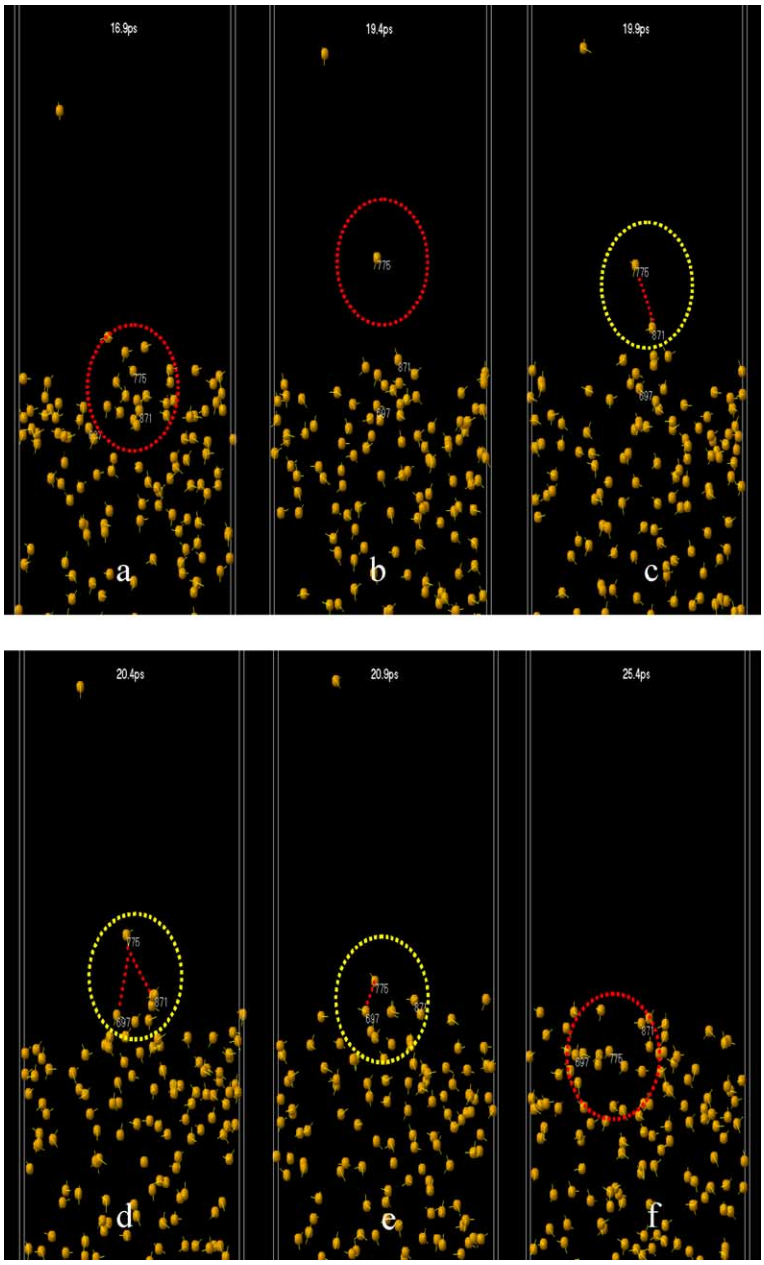


Fig. 8. Effect of hydrogen bond on the molecular behavior near the interface.

hydrogen bond effect is found to be more significant at low temperatures than at high temperatures. Indeed, the coordination number of water molecules due to hydrogen bond is found to decrease with increasing temperature as shown in Fig. 9. At higher temperatures, the possibility of coordination number less than 3 is significantly increased. This may be due to a higher mean velocity at high temperatures than that at low temperatures.

Molecular exchanges may also take place in the interface region. A vapor molecule condenses on the interface may release its energy to a nearby molecule in the interface and make that molecule evaporate. Fig. 10 shows a case of the molecular exchange processes in the interface. At 137.4 ps, No. 591 molecule in the vapor region is moving toward the interface. After about 13 ps of interactions in the interface region, No. 302 molecule in the interface is ejected into the vapor region. Such a kind of molecular exchange phenomenon was reported earlier by Motsumoto [5] through molecular dynamics simulations.

### 3.3. Evaporation of thin liquid film into vacuum

The results of simulation illustrates that the evaporation of the thin liquid film into a closed vacuum space leads to rapid increase of vapor atoms initially in the vacuum (vapor) side. Finally an asymptotic value corresponding to the equilibrium state is approached, as shown in Fig. 11 for water film evaporation at 403.15 K. Significant fluctuations of molecular density in the vapor region is present. Each point of the curve shown in the figure is that after integration from $t = 0$ to the time of that data point. Relatively large oscillations are still present. In particular, significant oscillations in vapor side atom density exist even after the equilibrium state is approached. This suggests a dynamic equilibrium at the interface, i.e., the evaporation rate is larger than the condensation rate at one time and smaller at the other time. This is contrary to the common view that the evaporation rate is exactly equal to the condensation rate after an equilibrium state is reached. The time evolution of molecular number density in the vapor side can be fitted very well by an asymptotic form as:

$$n(t) = C_1(1 - e^{-C_2 t}) \tag{7}$$

The above equation suggests that the net evaporation rate of liquid film into vacuum in a closed system may be modeled by the balance of evaporation and condensation rates as:

$$\frac{d}{dt}[Vn(t)] = A_i j_+ - A_i j_- \tag{8}$$

where $V$ is the volume of the vapor side, $A_i$ is the interfacial area, and $j_+$ and $j_-$ are the evaporation and condensation mass flux, respectively. Combined with the Schrage expression for $j_+$ and $j_-$ of interfacial mass transfer [15], the following equation for the evaporation coefficient can be obtained by the integration of Eq. (8) and subsequently equating with Eq. (7) [6]:

$$\sigma_e = \frac{C_1 C_2}{\left(\frac{A_i}{V}\right)\left(\frac{M}{2\pi R}\right)^{1/2}\frac{P_L}{T_L^{1/2}}} \tag{9}$$

Therefore, using the fitted parameters from the simulation results, the evaporation coefficient $\sigma_e$ can be evaluated by Eq. (9). In the above equation, $T_L$ and $P_L$ are the temperature and corresponding saturation pressure at the interface; $M$ and $R$ are the molecular weight and universal gas constant, respectively.

Fig. 12 shows a comparison of the evaporation coefficient obtained in the present work with several theoretical predictions in the literature [16–19], which were reviewed in Marek and Straub [2]. The evaporation coefficients thus evaluated are from 0.3 to 0.6 and increase with increasing the pressure (and thus the corresponding saturated temperature) in the pressure range from 0.6 to 20 bar. As discussed earlier in Section 3.2, the hydrogen bond effect, which tends to recapture some of the molecules just evaporated with slow speed back to the interface region, becomes less significant at high temperatures. As a result, the evaporation coefficient increases with increasing pressure and corresponding saturation temperature. Such a pressure or temperature effect is consistent with theoretical predictions on condensation coefficient in the literature [2]. The figure also illustrates that the condensation coefficients predicted in the literature is significantly higher than the evaporation coefficient predicted in the present study. This trend is also consistent with the analysis of Marek and Straub [2].

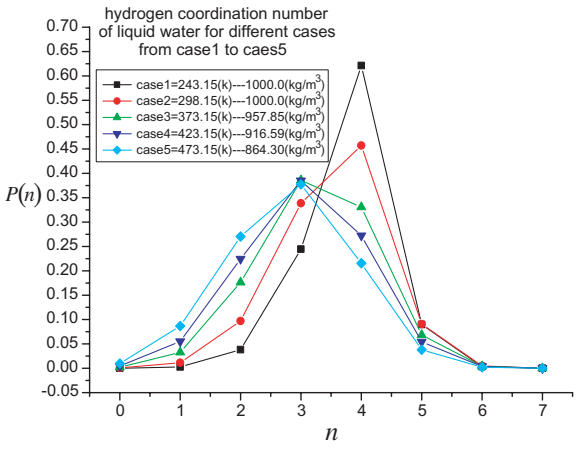


Fig. 9. Hydrogen coordination number distribution for water at different temperatures.

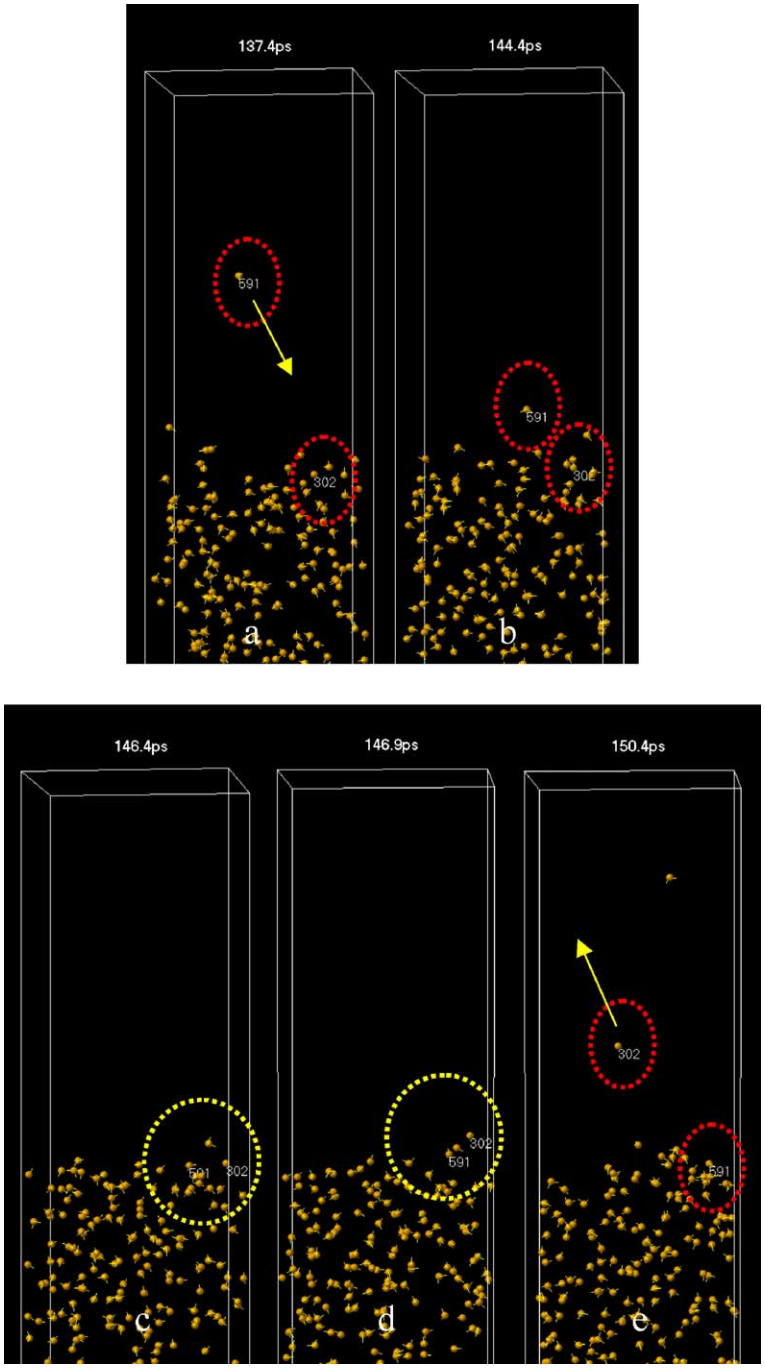


Fig. 10. Molecular exchange processes at of near the interface.

## 4. Conclusions

Molecular dynamics simulations are conducted for the evaporation of a thin liquid water layer into vacuum. The following conclusions may be drawn from the results of the present study.

1. The density profile near the interface may be fitted very well by a hyperbolic tangent function as suggested in the literature. The thickness of the interfacial region increases approximately linearly with increase in temperature.

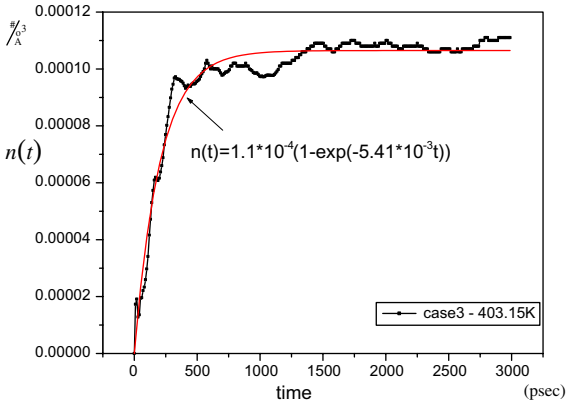


Fig. 11. Time evolution of molecular density in the vapor region due to thin water layer evaporation at 403.15 K.

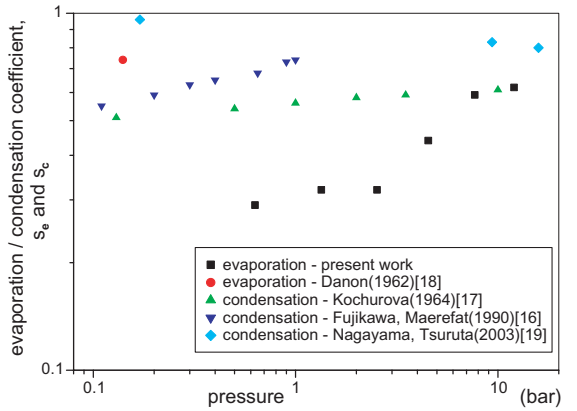


Fig. 12. Evaporation coefficient of water at various pressure.

2. Molecular dynamics simulations demonstrate that the mean temperature at the interface is lower than that in the liquid layer due to the escape of more energetic, vapor-like molecules from the interface to the vapor region. On the other hand, the temperature fluctuations in the interface region are much more violent than that inside the liquid layer, partially because the molecules in the interface region are less constraint than those inside the liquid.
3. The molecular dynamics may reveal molecular behavior near or in the interface region. The hydrogen bond effects may recapture the molecules just evaporated and reduce the evaporation coefficient. Such an effect is weakened with increasing temperature or corresponding saturation pressure.
4. The combination of molecular dynamics simulations and the classical Schrage model for the interface mass transfer provide an elegant and quick way to determine the evaporation coefficient. The evaporation coefficient thus determined compares fairly well with, but smaller than, the theoretical predictions of condensation coefficient reported in the literature.

## Acknowledgments

This work was supported by the National Science Council of Taiwan under the contract no. of NSC 90-2212-E-007-103. The authors would also like to acknowledge the valuable discussion with Dr. M.H. Hsieh of the Institute of Nuclear Energy Research, Taiwan, ROC. The computer program was executed using the IBM p690 workstations provided by the National Center for High-Performance Computing, Taiwan, ROC. The free image program PV-WIN employed in the present study for displaying the molecular behavior near or at the interface, Figs. 6–8, was downloaded from the website of Prof. Shigeo Maruyama of the Department of Mechanical Engineering, University of Tokyo.

## References

[1] T. Ytrehus, Molecular-flow effects in evaporation and condensation at interfaces, Multiphase Sci. Technol. 9 (1997) 205–327.
[2] R. Marek, J. Straub, Analysis of the evaporation coefficient and the condensation coefficient of water, Int. J. Heat Mass Transfer 44 (2001) 39–53.
[3] V.P. Carey, Modeling of microscale transport in multiphase system, Proc. 11th Int. Heat Transfer Conference 1 (1998) 23–40.
[4] K. Yasuoka, M. Matsumoto, Molecular simulation of evaporation and condensation. I. Self condensation and molecular exchange, Proc. ASME/JSME Thermal Eng. Conf. 2 (1995) 459–464.
[5] M. Matsumoto, Molecular dynamics of fluid phase change, Fluid Phase Equilibria 144 (1998) 307–314.
[6] Y.W. Wu, C. Pan, Molecular dynamics simulation of evaporation of a thin liquid argon layer in a closed system, Paper HT 2003-47217, 2003 ASME Summer Heat Transfer Conference, Las Vegas, July 20–23.
[7] P. Yi, D. Poulikakos, J. Walther, G. Yadigaroglu, Molecular dynamics simulation of evaporation of an ultra-thin liquid argon layer on a surface, Int. J. Heat Mass Transfer 45 (2002) 2087–2100.
[8] Y.W. Wu, C. Pan, A molecular dynamics simulation of bubble nucleation in homogeneous liquid under heating with constant mean negative pressure, Microscale Thermophys. Eng. 7 (2003) 137–151.
[9] J.M. Haile, Molecular Dynamics Simulation, Wiley, New York, 1992, pp. 40–43.
[10] S. Maruyama, Molecular dynamics method for microscale heat transfer, in: W.J. Minkowycz, E.M. Sparrow (Eds.), Advances in Numerical Heat Transfer, vol. 2, Taylor & Francis, New York, 2000, pp. 189–226, Chapter 6.

[11] Y.A. Cengel, M.A. Boles, Thermodynamics an Engineering Approach, third ed., The McGraw-Hill Companies, New York, 1998, pp. 904–908.
[12] J. Alejandre, D.J. Tildesley, G.A. Chapela, Molecular dynamics simulation of the orthobaric densities and surface tension of water, J. Chem. Phys. 102 (1995) 4574–4583.
[13] J.L. Rivera, M.P. Predota, A.A. Chialvo, P.T. Cummings, Vapor–liquid equilibrium simulations of the SCPDP model of water, Chem. Phys. Lett. 357 (2002) 189–194.
[14] G.A Chapela, G. Saville, S.M. Thompson, J.S. Rowlinson, Computer simulation of a gas–liquid surface, Part 1, J. Chem. Soc. Faraday Trans. II 8 (1977) 1133–1144.
[15] R.W. Schrage, A Theoretical Study of Inter-phase Mass Transfer, Columbia University Press, New York, 1953.
[16] S. Fujikawa, M. Maerefat, A study of the molecular mechanism of vapor condensation (in Japanese), Trans. JSME 56 (1990) 1376–1384 , translation in:, JSME Int. J. 33 (4) (1990) 634–641.
[17] N.N. Kochurova, The problem of condensation coefficients, Int. Chem. Eng. 4 (4) (1964) 603–605.
[18] F. Danon, Topics in Statistical Mechanics of Fluids, Ph.D. thesis, University of California, UCRL-10029, 1962.
[19] G. Nagayama, T. Tsuruta, A general expression for the condensation coefficient based on transition state theory and molecular dynamics simulation, J. Chem. Phys. 118 (2003) 1392–1399.